Volume electron microscopy for neuronal circuit reconstruction

Kevin L Briggman[1] and Davi D Bock[2]

The last decade has seen a rapid increase in the number of tools to acquire volume electron microscopy (EM) data. Several new scanning EM (SEM) imaging methods have emerged, and classical transmission EM (TEM) methods are being scaled up and automated. Here we summarize the new methods for acquiring large EM volumes, and discuss the tradeoffs in terms of resolution, acquisition speed, and reliability. We then assess each method's applicability to the problem of reconstructing anatomical connectivity between neurons, considering both the current capabilities and future prospects of the method. Finally, we argue that neuronal 'wiring diagrams' are likely necessary, but not sufficient, to understand the operation of most neuronal circuits: volume EM imaging will likely find its best application in combination with other methods in neuroscience, such as molecular biology, optogenetics, and physiology.

Addresses
[1] Circuit Dynamics and Connectivity Unit, National Institute of Neurological Disorders and Stroke, National Institutes of Health Bethesda, MD, USA
[2] Janelia Farm Research Campus, Howard Hughes Medical Institute, Ashburn, VA, USA

Corresponding authors: Briggman, Kevin L (briggmankl@mail.nih.gov) and Bock, Davi D (bockd@janelia.hhmi.org)

Introduction

Vertebrate and invertebrate nervous systems are densely packed with intertwining neuronal axons and dendrites and the synapses between them. The small physical size of these structures, as thin as 40–50 nm in diameter [1,2], requires imaging by electron microscopy (EM), particularly when the goal is the dense reconstruction of neuronal circuits. By imaging volumes of brain using 3-dimensional EM, the details of neuronal shape and connectivity can be reconstructed. Importantly, and in contrast to fluorescence-based labeling approaches that require sparse labeling [3] or super-resolution optical imaging [4,5] to resolve densely packed neurites, standard EM stains result in a relatively unbiased staining of all membranes and synapses in the neuropil [6]. This means

that EM volumes can, in principle, be used to reconstruct the complete connectivity of a neuron with all its presynaptic and postsynaptic partners. Furthermore, this operation can be repeated for all the neurons in the volume, such that the connectivity of the neurons comprising a circuit — its wiring diagram or 'connectome' — can be extracted.

The main challenge in volume EM imaging is to acquire a data set of sufficient size, resolution, and completeness that the tortuous trajectories of axons and dendrites can be followed, and the chemical (and, ideally, electrical) synaptic connections identified. The necessary volume depends on the anatomical extent of the circuit to be characterized. For example, the volume of an entire adult nematode, *Caenorhabditis elegans* (approximately 50 μm × 50 μm × 1000 μm, [7]), is about 1% that of a single mouse cortical column (400 μm × 400 μm × 1000 μm, [8]). The required 3D voxel resolution depends on how fine the processes are that must be traced: the finer the process, the greater the required resolution to reliably follow it over a long distance. For example, dendritic spine necks in the mammalian central nervous system can be as fine as 40 nm in diameter [2], and the fine neurites of the fruit fly *Drosophila melanogaster* can be as thin as 50 nm in diameter [1]. The required completeness of the EM-imaged volume is related to required resolution: when image data are lost due to staining artifacts, a missed section, or some other glitch in the imaging process, the probability of ambiguities in the dataset increases, resulting in fine processes becoming lost or mixed up during tracing.

There is currently no 'best' volume EM imaging method. Rather, each of the available methods involves tradeoffs in size, resolution and completeness, and which method is most appropriate depends on the scientific questions under investigation. The field, however, is changing rapidly. Here we summarize current volume EM methods, focusing on those designed to answer questions about neuronal circuit structure, and offer suggestions about the types of circuit questions that each method is currently well suited to answer.

Acquisition techniques

The primary dichotomy between modern volume EM methods lays in the choice of widefield transmission electron microscopy (TEM)-based or scanning electron microscopy (SEM)-based techniques. Because TEM-based approaches rely on the imaging of those electrons that pass through a specimen, a requirement is the use of thin sections cut before imaging. SEM, in contrast, is

2 **Neurotechnology**

typically used to image electrons backscattered from the surface of samples, allowing the surfaces of both thin sections and block-faces to be imaged. Both types of instrument are capable of high lateral (x–y) resolutions down to a few nanometers, a resolution sufficient for circuit reconstruction.

However, the z-resolution of all techniques (with the exception of electron tomography [9]) depends on the ability to remove thin sections from a block of plastic embedded tissue. The majority of the new technical developments we focus on are aimed at improving this minimum z-resolution or, at least, improving the reliability of thin sectioning. Since the lateral resolution is typically several-fold finer than the section thickness, z-resolution imposes one important limit on the usefulness of datasets.

TEM-based methods

In modern serial section TEM (ssTEM [10••]), individual thin sections, typically between 40 and 90 nm in thickness (e.g. [11•,12,13]) are cut in an ultramicrotome with a diamond knife (Figure 1a). Sections are picked up by hand onto a 3 mm diameter metal support grid. The grid typically has a slot of length 2 mm, and width 0.2–1 mm. An electron-transparent support film is suspended across the slot, and the thin sections are picked up onto the film. To enhance contrast, the sections are usually post-stained with heavy metals. The grid is then manually inserted into a TEM, and a small (typically 10–20 μm) region of interest is selected for imaging. Electrons are accelerated using an 80–120 kV potential, permitting them to pass through the sample and underlying support film. Some electrons are scattered by the heavy metals in the sample, generating contrast. After passing through a series of electromagnetic enlarger lenses, the transmitted electron image reaches a layer of phosphor, and a digital camera is used to acquire EM images (Figure 1a). TEM imaging is inherently parallel, with each pixel on the camera corresponding to a location in the section. With digital TEM cameras, large image mosaics can be conveniently collected through the use of a motorized x–y stage to translate the sample between image acquisitions, allowing the entire section area to be imaged.

The upper limit for section size in routine ssTEM is 1 mm × 2 mm, the dimensions of the slot in the support grid. Although custom grids with slots up to 25 mm long have been used (e.g. [14], p. 60), the prospects for increased section width in ssTEM are limited by the fragility of the support film underlying the cut sections and the narrowness of the gap in the objective lens pole piece which admits the sample holder.

SEM-based methods

In a SEM, a finely focused electron beam is raster scanned across the surface of a sample and backscattered electrons are collected with a detector positioned above the sample (Figure 1b–d). Unlike TEM-based imaging, SEM-based imaging is therefore inherently serial. The use of low electron energies (typically 1–3 kV) limits the depth of the back-scattered electron signal to the upper tens of nanometers of the sample [15]. Therefore, both thin sections and block faces can be imaged with high z-resolution. As in TEM-based methods, following the acquisition of one field of view (typically tens of microns on a side), an x–y stage translates the sample within the SEM, allowing large millimeter-sized mosaics to be imaged.

An automated tape-collecting ultramicrotome (ATUM) has been recently developed to automate the pickup of sections onto a spool of support tape (Figure 1b) [16•]. This technique obviates the specialized and error-prone process of manual sectioning, and provides the additional benefit of cutting sections thinner (30 nm, K. Hayworth, personal communication) than what is routinely possible in conventional ssTEM. Additionally, much wider and longer sections than normal — up to 2.5 mm × 6 mm — can be cut (K. Hayworth, personal communication), permitting unusually large brain volumes to be thin-sectioned. The use of an electron opaque support tape, however, means that sections collected with ATUM cannot be imaged within a TEM, but rather must use the secondary or backscattered electron signal in a SEM (Figure 1b) [17••].

Alternatively, the surface of tissue blocks can be imaged in SEMs and sectioned *in situ* within the SEM vacuum chamber [18••,19]. Ideally, the energy-dependent electron sampling depth is matched to the thickness of tissue that is then removed. Tissue can be removed either mechanically using a diamond knife, as with serial block-face SEM (SBEM, Figure 1c [18••]) or by milling with a focused ion beam (FIB-SEM, Figure 1d [20••,21•]). The cycle of obtaining block-face images and then cutting/milling is fully automated, with no interaction from the experimenter. Unlike ssTEM and ATUM-SEM, block-face SEM methods are destructive; the sections are lost as soon as they are removed from the block face.

Resolution and reliability

The lateral resolutions obtainable in TEMs remain unparalleled, with sub-nanometer resolutions easily achieved in modern TEMs. In practice, sub-nanometer imaging is overkill for the purposes of circuit reconstruction; a common pixel resolution in TEM is ∼2–4 nm (e.g. [11•,12,13]). Such resolutions are also achievable in SEMs where the size of the electron probe ultimately limits resolutions to 1–2 nm [22]. What resolution do we need for circuit reconstruction? If the minimum diameter of a neurite, such as a spine neck, can be expected to be as thin as 40–50 nm [1,2], the maximum voxel size in any

Figure 1

Current Opinion in Neurobiology
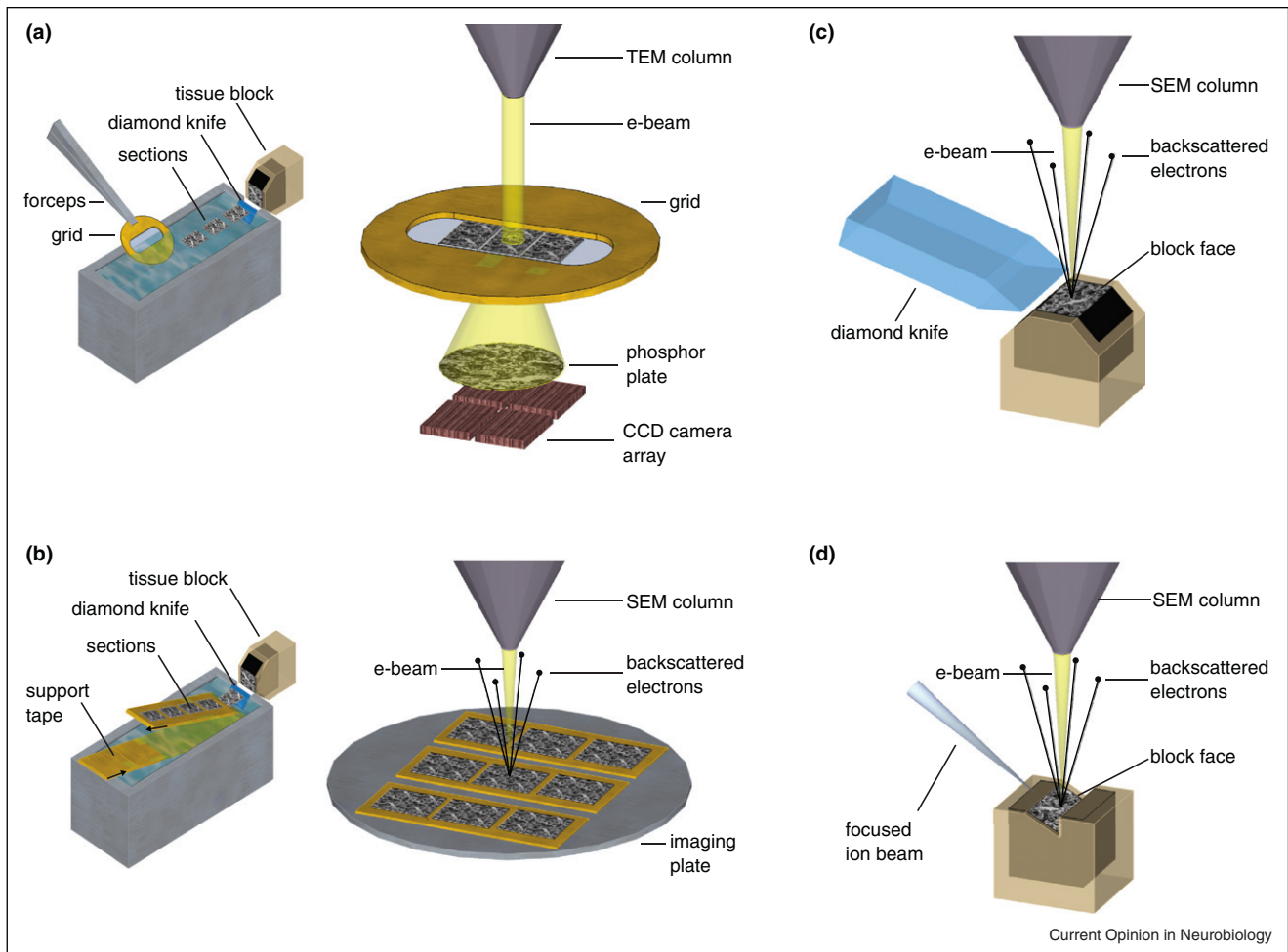
Simplified schematics (not to scale) of the volume EM techniques described in this review. **(a)** Serial section transmission electron microscopy (ssTEM). Sections are cut by hand with an ultramicrotome, floated onto a water boat, and picked up onto grids. In ssTEM, electrons transmitted through the sample are focused with electron optics (not pictured) to form an image on a phosphor plate and the image is recorded digitally with, in this case, a CCD camera array (TEMCA). **(b)** Automated tape-collecting ultramicrotome scanning electron microscopy (ATUM-SEM). Sections are cut automatically on an ultramicrotome and collected from the water bath using a custom designed tape-collection conveyor belt. Because the support tape is electron opaque, ATUM sections are mounted on an imaging plate and imaged in a SEM. Images are formed by collecting back-scattered electrons with an electron detector mounted above the sample (not shown). **(c)** Serial block-face scanning electron microscopy (SBEM). Automated sectioning with a diamond knife and imaging are performed within the vacuum chamber of a SEM using a custom designed microtome and specimen stage. **(d)** Focused ion beam milling scanning electron microscopy (FIB-SEM). Automated milling with a focused ion beam and imaging are performed within a dual-beam SEM.

dimension should ideally be at least half as thick (i.e. 20–25 nm) to reliably follow every neurite. However, much higher resolutions of 3–5 nm are in principle required for the reliable detection of some types of subcellular structures such as gap junctions [23].

The new techniques are distinguished by improved z-resolutions (Figure 2). FIB-SEM [20••] currently offers the highest z-resolution of 5 nm (Figure 3). Automated serial sectioning using diamond knives, either with SBEM or ATUM-SEM, can lead to repeatable sectioning of 20–30 nm [24•]. Manual sectioning using an ultramicrotome

as in ssTEM is typically limited to sections of 40–50 nm [10••]. z-Resolution in TEM can be improved to a few nanometers through tomographic reconstruction, in which the same field of view is imaged at multiple small tilt increments [9]. The number of tilts typically used for EM tomography would be prohibitively slow for volume EM imaging of circuits. However, a recent method of sparse tomographic reconstruction [25•], in which z-resolution is moderately improved using only a few tilt angles, may permit ssTEM methods to achieve z-resolution comparable to that of SBEM or ATUM-SEM. Sparse tilts in combination with re-imaging at high magnification

Figure 2
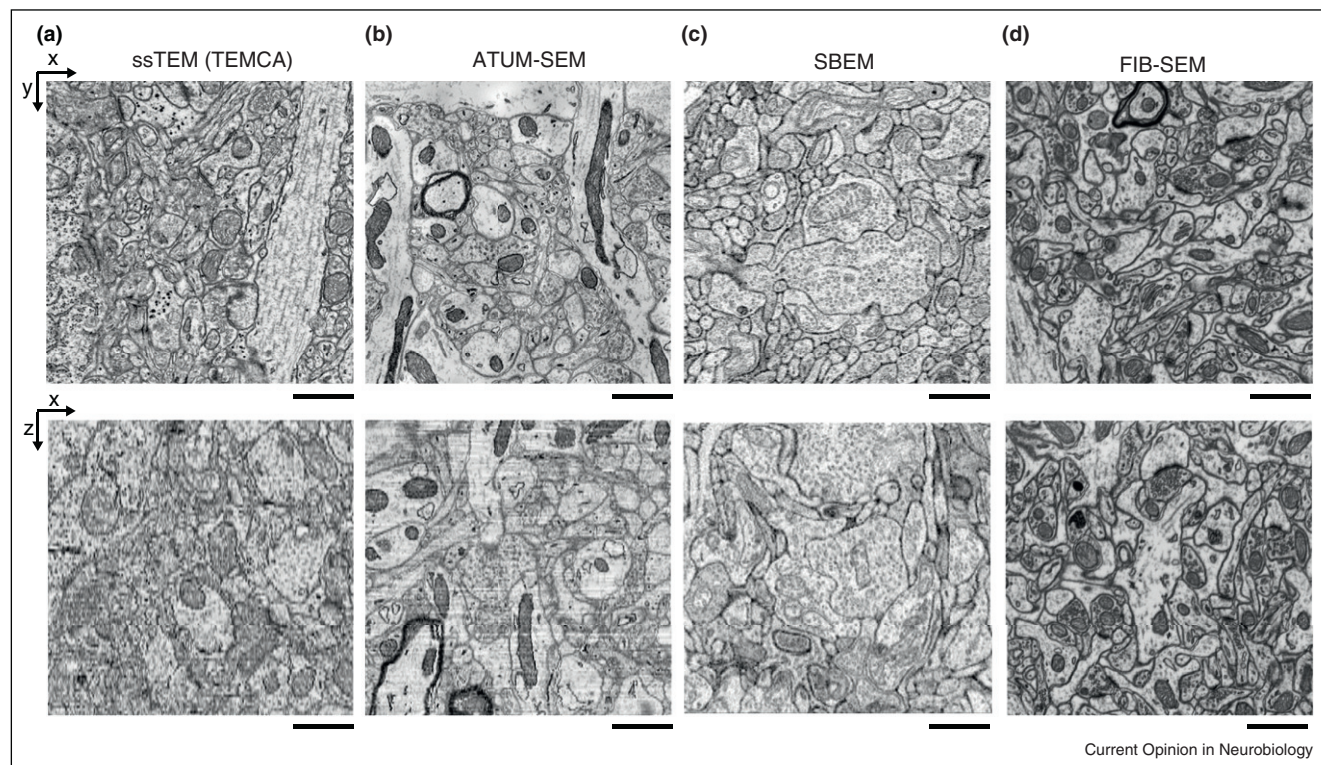
3D volumes acquired using each of the techniques displayed as original *x–y* images and *x–z* reslices through the volumes after digital alignment. **(a)** ssTEMCA: layer 2/3 of mouse visual cortex imaged at 4 nm × 4 nm × 45 nm. **(b)** ATUM-SEM: mouse cortex imaged at 3 nm × 3 × 29 nm. **(c)** SBEM: inner plexiform later of mouse retina imaged at 12 nm × 12 nm × 25 nm. **(d)** FIB-SEM: mouse cortex imaged at 5 nm × 5 nm × 5 nm. Images courtesy of D. Bock (a), J. Lichtman (b), K. Briggman (c), and G. Knott (d). Scale bars 1 μm.

(0.2 nm *x–y* resolution) can also be used to disambiguate gap junctions from chemical synapses and other membrane appositions [13].

There is currently a spectrum of opinion regarding the importance of high z-resolution. Some researchers have suggested that a high enough *x–y* resolution allows most neurites to be followed unambiguously even with modest z resolutions of 45–50 nm [11•,12,26]. Others stress the importance of achieving nearly isotropic voxels, not only for the ability to follow *every* neurite within a dataset, but also for the development of automated image segmentation algorithms [27]. To date, a comprehensive assessment of the degree to which neuron traceability is compromised by the limited z resolution of all techniques has not been performed.
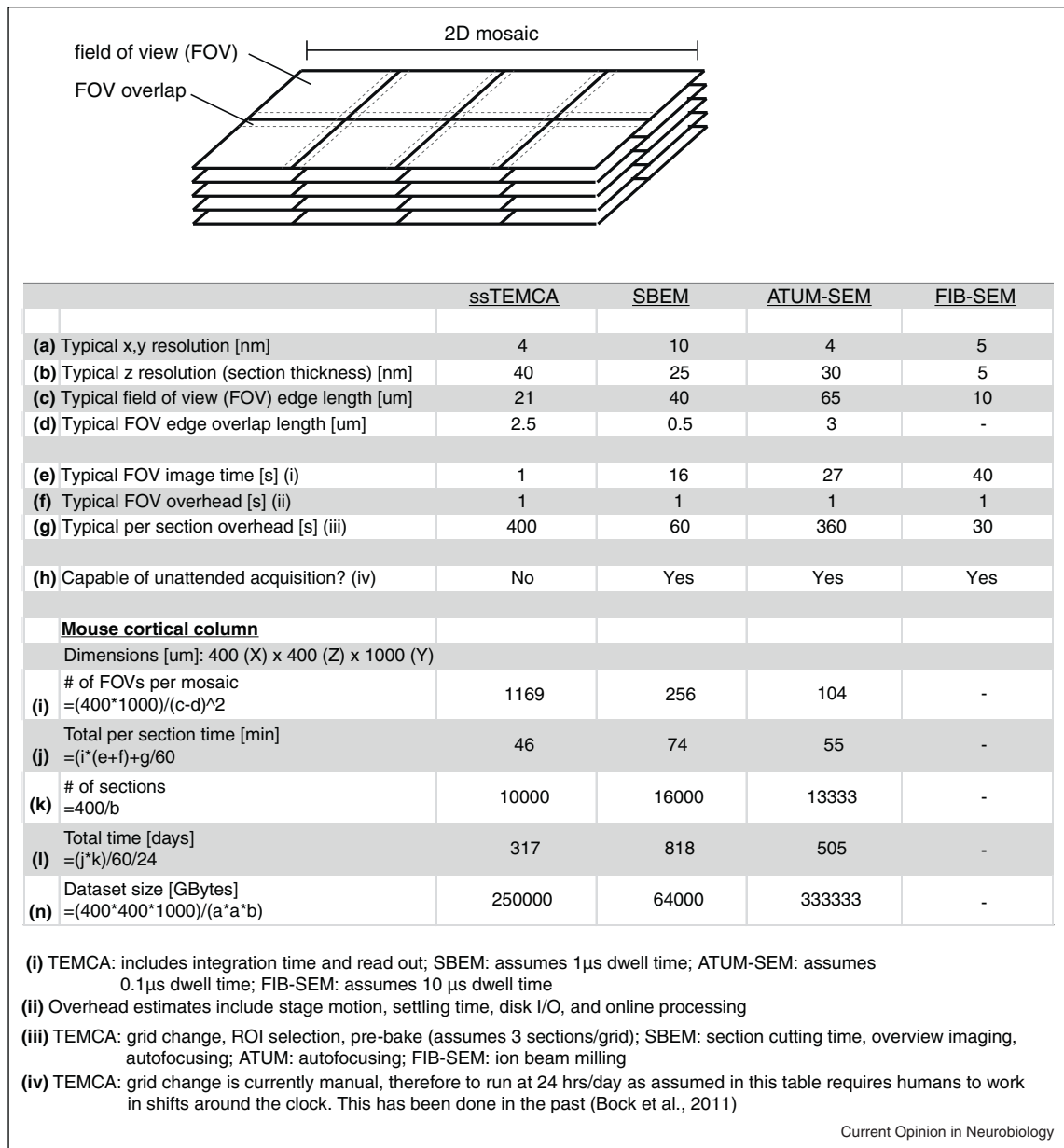
A limitation of manual sectioning remains that some sections inevitably suffer from folds or warping during cutting or post-staining. These errors in the final dataset can be minor (many neurite continuities are traceable across a single missed section [11•]), although a rigorous analysis of the effects of missed or damaged sections has not been published. Manual sectioning methods also generally suffer from variability in section thickness, making it difficult to directly compare average z-resolutions. The automated sectioning methods (ATUM-SEM and SBEM) were designed with an increase in the repeatability of section thickness in mind. Again, however, a quantitative comparison of section thickness variability between the various methods has not yet been performed.

Acquisition speed

Because local neuronal circuits can span 3D volumes of at least hundreds of microns on a side, acquisition speed has become an increasingly important parameter (Figure 3). A TEM camera array (TEMCA, Figure 1a) enabled high acquisition rates through the use of multiple high frame rate cameras in combination with optimized stage motion and on-line image processing software [11•]. System throughput is largely determined by how quickly image frames can be read out from the cameras in the array, and how quickly the sample can be moved between image frame acquisitions. Saturating the camera sensors in the short period of a single frame exposure can require a large electron dose (electrons/nm^2). To avoid rupturing the thin section and its underlying support film with the intense electron beam, various optimizations in sample

Figure 3

	ssTEMCA	SBEM	ATUM-SEM	FIB-SEM
(a) Typical x,y resolution [nm]	4	10	4	5
(b) Typical z resolution (section thickness) [nm]	40	25	30	5
(c) Typical field of view (FOV) edge length [um]	21	40	65	10
(d) Typical FOV edge overlap length [um]	2.5	0.5	3	-
(e) Typical FOV image time [s] (i)	1	16	27	40
(f) Typical FOV overhead [s] (ii)	1	1	1	1
(g) Typical per section overhead [s] (iii)	400	60	360	30
(h) Capable of unattended acquisition? (iv)	No	Yes	Yes	Yes
Mouse cortical column				
Dimensions [um]: 400 (X) x 400 (Z) x 1000 (Y)				
(i) # of FOVs per mosaic =(400*1000)/(c-d)^2	1169	256	104	-
(j) Total per section time [min] =(i*(e+f)+g/60	46	74	55	-
(k) # of sections =400/b	10000	16000	13333	-
(l) Total time [days] =(j*k)/60/24	317	818	505	-
(n) Dataset size [GBytes] =(400*400*1000)/(a*a*b)	250000	64000	333333	-

(i) TEMCA: includes integration time and read out; SBEM: assumes 1µs dwell time; ATUM-SEM: assumes 0.1µs dwell time; FIB-SEM: assumes 10 µs dwell time

(ii) Overhead estimates include stage motion, settling time, disk I/O, and online processing

(iii) TEMCA: grid change, ROI selection, pre-bake (assumes 3 sections/grid); SBEM: section cutting time, overview imaging, autofocusing; ATUM: autofocusing; FIB-SEM: ion beam milling

(iv) TEMCA: grid change is currently manual, therefore to run at 24 hrs/day as assumed in this table requires humans to work in shifts around the clock. This has been done in the past (Bock et al., 2011)

Current Opinion in Neurobiology

Large 3D EM volumes require overlapping fields of view to form 2D mosaics of each section. The time to acquire each FOV and the overhead for each mosaic and section varies for the different techniques. Typical values for each technique are intended to serve only as estimates. Given these estimates, the duration of an experiment to acquire a volume the size of a mouse cortical column (TEM or SEM) are provided in the table. Note that the required voxel resolution will be dependent on characteristics of the tissue under examination, for example, minimum neurite diameter and staining contrast. Values courtesy of D. Bock (ssTEMCA), K. Hayworth and J. Lichtman (ATUM-SEM), K. Briggman (SBEM), and G. Knott (FIM-SEM).

preparation are important, including carbon coating of the support film, minimization of post-staining artifact, and elimination of any inhomogeneity in the support film. Electron dose must also be monitored with SBEM and FIB-SEM, to prevent too much electron-beam induced damage to the block-face before section removal (although the tolerable dose may be different for SBEM and FIB-SEM). The imaging speed of SEM-based approaches is limited by the bandwidth of electron detectors and the available electron beam current leading to a tradeoff between the acquisition rate and the signal-to-noise ratio of images. In addition to raw image acquisition speed, the duration of an experiment is extended by time spent sectioning, loading and unloading specimens from vacuum, and translating samples under the electron beam to construct image mosaics (Figure 3). For large volumes,

the duration of these steps can sum to substantial over-head (see actual time estimates, Figure 3).

Post-acquisition alignment
Once a series of images has been acquired, an alignment step is necessary to stitch the images into a 3D volume. An advantage of block-face SEM imaging is the inherent registration that comes with acquiring images before sectioning; typically only a simple translational shift of images is required [24•]. Alignment is more complicated for ssTEM and ATUM-SEM sections, often requiring local warping algorithms to compensate for section stretching, folds in sections, and distortions that occur during imaging. While such alignment procedures were, historically, daunting, the use of high-performance computing makes automating complex alignment algorithms possible [11•,28,29].

Tissue preparation and correlative techniques
The electron dense staining of tissue primarily still relies on chemical compounds first described decades ago during the early years of biological EM. Stains based on high-Z number elements such as osmium, uranium, and lead are most common for each of the techniques described [30]. The use of *en bloc* staining methods [30] is, in particular, essential for the block-face methods in which post-staining of sections is not possible. But the art of staining is by no means dead. The development of indicators to highlight structures of interest, such as membrane-targeted HRP [31,32] or genetically encoded fluorescent reactive oxygen generators for photoconversion [33] is geared toward selectively increasing contrast in genetically controllable ways.

While electron micrographs provide structural information at resolutions unreachable by light microscopy, correlative light microscopy can provide the labeling necessary to bridge the gap to both circuit function and patterns of molecular expression and localization. Array tomography was developed to take advantage of the z resolution of ultrathin sections combined with the ability to multiplex the labeling of antigens [34]. By sequentially exposing a section to fluorescently labeled antibodies, a number of different synaptic proteins (for example) can be localized to the same synapse [35]. The tissue processing steps needed to label endogenous antigens are, however, often incompatible with good ultrastructural preservation; nevertheless, the labeling of experimentally introduced antigens has been demonstrated with good preservation of ultrastructure [36,37]. Additionally, near-infrared branding can be used to place a high-resolution fiducial mark near a fluorescent object of interest, for visualization using both light and EM [38].

Another approach to connect circuit function to structure is to directly measure the activity of populations of neurons from the same piece of tissue to be reconstructed.

Methods for 2-photon laser scanning calcium imaging [39] allow signals from neurons hundreds of microns deep within the brain to be recorded without the risk of damaging ultrastructure with recording electrodes. When combined with subsequent volume EM acquisitions, patterns in wiring diagrams can be directly correlated with neuronal activity [11•,24•].

Current best applications and future outlook
Each volume EM method has a maximum section size. ATUM-SEM sections are supported by a tape substrate, and can therefore be as large as 2.5 mm × 6 mm (K.J. Hayworth, pers. comm.). Sections cut for TEM can be as large as 1 mm × 2 mm, with the possibility of longer sections if custom support grids (e.g. [14], p. 60) are used. SBEM, in its current implementation, is limited to tissue blocks of about 1 mm on a side [18••], although there is no fundamental technological limit to acquiring larger volumes. For a variety of technical reasons, the spatial extent of FIB-SEM is limited to 50–100 μm per side.

Given these section dimensions and the resolutions described above, the techniques are currently best suited for different applications. Because FIB-SEM currently obtains the highest 3D resolution but is limited to small volumes, it is best suited for questions of local synaptic circuitry. SBEM is currently best suited for moderately sized (several hundred microns on a side) volumes containing circuits such as those within brain nuclei or perhaps cortical columns. ssTEM and ATUM-SEM, due to the current ability to cut and image the largest area sections, are best suited to multi-millimeter scale connectivity questions, perhaps even of whole brains of, for example, fruit flies or zebrafish larvae.

We anticipate that, as more labs begin to adopt these new techniques, a number of technical advances will follow. We anticipate further increases in z-resolution for each of the described techniques. For ssTEM, a more reliable sectioning and mounting procedure, possibly combined with ATUM technology, will likely aid data reliability. We also anticipate that the TEMCA approach offers substantial headroom for increased imaging throughput. The time estimates for each of the techniques provided in Figure 3 should therefore be taken only as current best estimates and are expected to significantly improve over the next few years.

Parallelizing acquisition across multiple microscopes is an obvious way to further increase throughput. When sections are cut before imaging as in ssTEM or ATUM-SEM, parallelization is straightforward: sections can be imaged in separate microscopes. Parallelizing block-face imaging between multiple microscopes is more difficult because the block would need to be cleaved in such a way to not lose any material along the cut. However, this may be possible using a recently described 'hot-knife' method [40].

Is it worth it?

As neuroscientists interested in the structure of circuits, a common question we are asked is something along the lines of: 'Will wiring diagrams tell us how circuits work?' Our answer is, 'Not on their own.' We argue that wiring diagrams, in the absence of any other information about cell type, synapse type, firing dynamics, etc. are likely *insufficient* to define circuit function. However, we think wiring diagrams may be *necessary* to understand circuit function. At a minimum, wiring diagrams in conjunction with complementary data will continue to generate, constrain, and falsify hypotheses about the functional organization of neural circuits.

We have mainly focused on methods for acquiring image data prerequisite to the determination of wiring diagrams, but wish to point out that data acquisition times, while daunting, are still miniscule compared to data analysis times for complete *dense* reconstruction [27]. In the short term, *sparse* reconstruction of a subset of the connections contained in vast image datasets will likely continue to yield new insights [11•,24•]. In the medium-to-long term, we anticipate that the recent progress in automating and speeding the acquisition of volume EM data will carry over to automation of the analysis of these large datasets [41,42], eventually permitting complete reconstruction of mammalian circuits across millimeter scales.

Acknowledgements

References and recommended reading

Papers of particular interest, published within the period of review, have been highlighted as:

- of special interest
- • of outstanding interest

1. Meinertzhagen IA, O'Neil SD: **Synaptic organization of columnar elements in the lamina of the wild type in *Drosophila melanogaster***. *J Comp Neurol* 1991, **305**:232-263.

2. Harris KM, Stevens JK: **Dendritic spines of CA 1 pyramidal cells in the rat hippocampus: serial electron microscopy with reference to their biophysical characteristics**. *J Neurosci* 1989, **9**:2982-2997.

3. Feng G, Mellor RH, Bernstein M, Keller-Peck C, Nguyen QT, Wallace M, Nerbonne JM, Lichtman JW, Sanes JR: **Imaging neuronal subsets in transgenic mice expressing multiple spectral variants of GFP**. *Neuron* 2000, **28**:41-45.

4. Betzig E, Patterson GH, Sougrat R, Lindwasser OW, Olenych S, Bonifacino JS, Davidson MW, Lippincott-Schwartz J, Hess HF: **Imaging intracellular fluorescent proteins at nanometer resolution**. *Science* 2006, **313**:1642-1645.

5. Klar TA, Jakobs S, Dyba M, Egner A, Hell SW: **Fluorescence microscopy with diffraction resolution barrier broken by stimulated emission**. *Proc Natl Acad Sci U S A* 2000, **97**:8206-8210.

6. Peters A, Palay SL, Webster Hd: *The Fine Structure of the Nervous System: Neurons and their Supporting Cells*. 3rd edn. New York: Oxford University Press; 1991.

7. Knight CG, Patel MN, Azevedo RB, Leroi AM: **A novel mode of ecdysozoan growth in *Caenorhabditis elegans***. *Evol Dev* 2002, **4**:16-27.

8. McCasland JS, Woolsey TA: **High-resolution 2-deoxyglucose mapping of functional cortical columns in mouse barrel cortex**. *J Comp Neurol* 1988, **278**:555-569.

9. Chen X, Winters CA, Reese TS: **Life inside a thin section: tomography**. *J Neurosci* 2008, **28**:9321-9327.

10. Harris KM, Perry E, Bourne J, Feinberg M, Ostroff L, Hurlburt J:
•• **Uniform serial sectioning for transmission electron microscopy**. *J Neurosci* 2006, **26**:12101-12103.
This review summarizes the current state of the art in ssTEM. Additionally, the authors provide essential advice to outsiders attempting to master the technique. Although newer methods have significant advantages, ssTEM remains a core technique for volume EM data acquisition, both in terms of potential imaging throughput and practical accessibility to a large population of neurobiologists.

11. Bock DD, Lee WC, Kerlin AM, Andermann ML, Hood G,
• Wetzel AW, Yurgenson S, Soucy ER, Kim HS, Reid RC: **Network anatomy and in vivo physiology of visual cortical neurons**. *Nature* 2011, **471**:177-182.
This article shows how volume EM and *in vivo* two-photon calcium imaging can be combined in mouse primary visual cortex. A custom high-speed TEM camera array was used to acquire a 450 μm × 350 μm × 50 μm EM volume. The EM data were used to determine the post-synaptic targets of the calcium-imaged neurons in the volume. Inhibitory interneurons in the volume were found to sample uniformly from the available surrounding excitatory pyramidal cells, without regard to orientation selectivity.

12. Cardona A, Saalfeld S, Preibisch S, Schmid B, Cheng A, Pulokas J, Tomancak P, Hartenstein V: **An integrated micro- and macroarchitectural analysis of the Drosophila brain by computer-assisted serial section electron microscopy**. *PLoS Biol* 2010, **8**:.

13. Anderson JR, Jones BW, Watt CB, Shaw MV, Yang JH, Demill D, Lauritzen JS, Lin Y, Rapp KD, Mastronarde D *et al.*: **Exploring the retinal connectome**. *Mol Vis* 2011, **17**:355-379.

14. Agar AW, Alderson RH, Chescoe D: *Principles and Practice of Electron Microscope Operation*. New York: American Elsevier; 1974.

15. Hennig P, Denk W: **Point-spread functions for backscattered imaging in the scanning electron microscope**. *J Appl Phys* 2007, **102**:.

16. Hayworth KJ, Kasthuri N, Schalek R, Lichtman J: **Automating the**
• **collection of ultrathin serial sections for large volume TEM reconstructions**. *Microsc Microanal* 2006, **12(Suppl. 2)**:86-87.
The authors introduce a method for automated sample collection in which serial thin sections cut by a conventional diamond knife are picked up from a water boat onto a thick, electron-opaque support tape. The tape is spooled into a reel, which is cut into easily handled segments. The method is able to cut much larger and thinner sections than is routinely possible in ssTEM.

17. Kasthuri N, Hayworth K, Lichtman J, Erdman N, Ackerley CA: **New**
•• **technique for ultra-thin serial brain section imaging using scanning electron microscopy**. *Microsc Microanal* 2007, **13**:26-27.
The authors demonstrate that the sections generated by the method of Hayworth *et al.* [16•] can be imaged using SEM, allowing semi-automated imaging of large sections at low resolution in combination with selected fields of view at high resolution.

18. Denk W, Horstmann H: **Serial block-face scanning electron**
•• **microscopy to reconstruct three-dimensional tissue nanostructure**. *PLoS Biol* 2004, **2**:e329.
The authors introduce an innovative method for volume EM data acquisition. A conventionally embedded block is placed in an SEM with a custom automated microtome. The surface of the block is scraped away with an oscillating diamond knife, and an SEM image of the resulting block face is acquired, in an iterative, completely automated fashion. This obviates error-prone manual pickup of serial sections (as for TEM) and simplifies the registration of volume EM image stacks, since image distortions are usually less than result from ssTEM.

19. Leighton SB: **SEM images of block faces, cut by a miniature microtome within the SEM — a technical note**. *Scan Electron Microsc* **(Pt 2)**:1981:73-76.

8 Neurotechnology

20. Knott G, Marchman H, Wall D, Lich B: **Serial section scanning**
•• **electron microscopy of adult brain tissue using focused ion beam milling**. *J Neurosci* 2008, **28**:2959-2964.
This paper demonstrates the successful application of the method of Heymann *et al.* [21•], FIB-SEM, for automated volume EM imaging of neural tissue. Although the volumes generated by this method are currently relatively small, the available *x*, *y*, and *z* resolutions are unsurpassed by any method besides conventional TEM tomography.

21. Heymann JA, Hayles M, Gestmann I, Giannuzzi LA, Lich B,
• Subramaniam S: **Site-specific 3D imaging of cells and tissues with a dual beam microscope**. *J Struct Biol* 2006, **155**:63-73.
The authors present focused ion beam SEM (FIB-SEM), a new method for volume EM imaging of biological tissue. A dual-beam electron microscope is used to alternately ablate a thin layer from the surface of a sample block with a beam of gallium ions, and then to image the surface of the block by SEM. Sectioning and imaging of the sample are completely automatic.

22. Goldstein J: *Scanning Electron Microscopy and X-ray Microanalysis*. 3rd edn.. New York: Kluwer Academic/Plenum Publishers; 2003.

23. Leitch B: **Ultrastructure of electrical synapses: review**. *Electron Microsc Rev* 1992, **5**:311-339.

24. Briggman KL, Helmstaedter M, Denk W: **Wiring specificity**
• **in the direction-selectivity circuit of the retina**. *Nature* 2011, **471**:183-188.
This article combined volume EM and two-photon calcium imaging in the mouse retina. SBEM was used to acquire a 350 μm $\times$ 300 μm $\times$ 60 μm volume, and the connections between starburst amacrine cells (SACs) and physiologically characterized direction-selective retinal ganglion cells (DSGCs) were reconstructed. SAC dendrites were found to inhibit DSGCs selectively: when the preferred direction of the SAC dendrite was aligned along the null direction of a DSGC, the probability of a SAC-DSGC synapse was greatly increased.

25. Veeraraghavan A, Genkin AV, Vitaladevuni S, Scheffer L, Xu S,
• Hess H, Fetter R, Cantoni M, Knott G, Chklovskii D: **Increasing depth resolution of electron microscopy of neural circuits using sparse tomographic reconstruction**. *2010 IEEE Conference on Computer Vision and Pattern Recognition (CVPR)*. 2010:1767-1774.
The authors demonstrate that the z resolution of conventional ssTEM can be increased by acquiring four additional tilt images at +45° and −45° on two perpendicular axes, and then processing the image stack using a set of basis functions which model membrane structure.

26. Mishchenko Y, Hu T, Spacek J, Mendenhall J, Harris KM, Chklovskii DB: **Ultrastructural analysis of hippocampal neuropil from the connectomics perspective**. *Neuron* 2009, **67**:1009-1020.

27. Helmstaedter M, Briggman KL, Denk W: **3D structural imaging of the brain with photons and electrons**. *Curr Opin Neurobiol* 2008, **18**:633-641.

28. Saalfeld S, Cardona A, Hartenstein V, Tomancak P: **As-rigid-as-possible mosaicking and serial section registration of large ssTEM datasets**. *Bioinformatics* 2010, **26**:i57-i63.

29. Tasdizen T, Koshevoy P, Grimm BC, Anderson JR, Jones BW, Watt CB, Whitaker RT, Marc RE: **Automatic mosaicking and volume assembly for high-throughput serial-section**

transmission electron microscopy. *J Neurosci Methods* 2010, **193**:132-144.

30. Hayat MA: *Principles and Techniques of Electron Microscopy: Biological Applications*. 4th edn.. Cambridge, UK/New York: Cambridge University Press; 2000.

31. Li J, Wang Y, Chiu SL, Cline HT: **Membrane targeted horseradish peroxidase as a marker for correlative fluorescence and electron microscopy studies**. *Front Neural Circuits* 2010, **4**:6.

32. Li J, Erisir A, Cline H: **In vivo time-lapse imaging and serial section electron microscopy reveal developmental synaptic rearrangements**. *Neuron* 2011, **69**:273-286.

33. Shu X, Lev-Ram V, Deerinck TJ, Qi Y, Ramko EB, Davidson MW, Jin Y, Ellisman MH, Tsien RY: **A genetically encoded tag for correlated light and electron microscopy of intact cells, tissues, and organisms**. *PLoS Biol* 2011, **9**:e1001041.

34. Micheva KD, Smith SJ: **Array tomography: a new tool for imaging the molecular architecture and ultrastructure of neural circuits**. *Neuron* 2007, **55**:25-36.

35. Micheva KD, Busse B, Weiler NC, O'Rourke N, Smith SJ: **Single-synapse analysis of a diverse synapse population: proteomic imaging methods and markers**. *Neuron* 2010, **68**:639-653.

36. Oberti D, Kirschmann MA, Hahnloser RH: **Correlative microscopy of densely labeled projection neurons using neural tracers**. *Front Neuroanat* 2010, **4**:24.

37. Oberti D, Kirschmann MA, Hahnloser RH: **Projection neuron circuits resolved using correlative array tomography**. *Front Neurosci* 2011, **5**:50.

38. Bishop D, Nikic I, Brinkoetter M, Knecht S, Potz S, Kerschensteiner M, Misgeld T: **Near-infrared branding efficiently correlates light and electron microscopy**. *Nat Methods* 2011, **8**:568-570.

39. Mittmann W, Wallace DJ, Czubayko U, Herb JT, Schaefer AT, Looger LL, Denk W, Kerr JN: **Two-photon calcium imaging of evoked activity from L5 somatosensory neurons in vivo**. *Nat Neurosci* 2011, **14**:1089-1093.

40. Hayworth KJ, Tapia JC, Kasthuri N, Schalek R, Lichtman J: In *Divide and Conquer — Lossless Thick Sectioning of Plastic-embedded Brain Tissue to Parallelize Large Volume Serial Reconstructions*. Edited by Planner NM. San Diego, CA: Society for Neuroscience; 2010. (Program No. 516.9).

41. Jain V, Bollmann B, Richardson M, Berger DR, Helmstaedter MN, Briggman KL, Denk W, Bowden JB, Mendenhall JM, Abraham WC *et al.*: **Boundary learning by optimization with topological constraints**. *2010 IEEE Conference on Computer Vision and Pattern Recognition (CVPR)*. 2010:2488-2495.

42. Helmstaedter M, Briggman KL, Denk W: **High-accuracy neurite reconstruction for high-throughput neuroanatomy**. *Nat Neurosci* 2011, **14**:1081-1088.